Hyperfine Interact (2016) 237:134
DOI 10.1007/s10751-016-1344-z

# Mössbauer spectroscopy of H, L and LL ordinary chondrites

**A. A. Maksimova[1] · M. I. Oshtrakh[1,2] · E. V. Petrova[1] · V. I. Grokhovsky[1] · V. A. Semionkin[1,2]**



**Abstract** Fifteen fragments of H, L and LL ordinary chondrites were studied using Mössbauer spectroscopy with a high velocity resolution at 295 K. A new approach to fit troilite magnetic sextet using simulation of the full static Hamiltonian was applied that decreased spectra misfits. This approach permitted to obtain more correct and reliable parameters for the minor spectral components. Small variations in the $^{57}$Fe hyperfine parameters were revealed for the M1 and M2 sites in both olivine and orthopyroxene as well as for $\alpha$-Fe(Ni, Co), $\alpha_2$-Fe(Ni, Co) and $\gamma$-Fe(Ni, Co) phases in different ordinary chondrites. Some Mössbauer parameters showed the possibility to distinguish ordinary chondrites from H, L and LL groups that may be useful for their systematics.

**Keywords** Mössbauer spectroscopy · H · L and LL ordinary chondrites · Hyperfine interactions · Systematics of ordinary chondrites

## 1 Introduction

Meteorites are the unique material for investigation due to its unique structure formed in the extreme space conditions which cannot be reproduced at Earth. There are three groups of meteorites (within the coarse classification) such as stony meteorites, iron meteorites

This article is part of the Topical Collection on *Proceedings of the 2nd Mediterranean Conference on the Applications of the Mössbauer Effect (MECAME 2016), Cavtat, Croatia, 31 May-3 June 2016*

✉ M. I. Oshtrakh
oshtrakh@gmail.com

1 Department of Physical Techniques and Devices for Quality Control, Institute of Physics and Technology, Ural Federal University, Ekaterinburg, 620002, Russian Federation

2 Department of Experimental Physics, Institute of Physics and Technology, Ural Federal University, Ekaterinburg, 620002, Russian Federation

Published online: 27 September 2016

and stony-iron meteorites. Ordinary chondrites belong to the former group and are considered as peers of the Solar system. They are characterised by the presence of olivine $(Fe, Mg)_2SiO_4$, orthopyroxene $(Fe, Mg)SiO_3$ clinopyroxene $(Fe, Mg, Ca)SiO_3$, troilite FeS, chromite $FeCr_2O_4$, $\alpha$-Fe(Ni, Co), $\alpha_2$-Fe(Ni, Co) and $\gamma$-Fe(Ni, Co) metallic phases, etc. Therefore, the presence of the iron-bearing phases allows applying $^{57}$Fe Mössbauer spectroscopy in the study of ordinary chondrites (see, for instance, [1–4]). Ordinary chondrites are subdivided into three groups (H, L and LL) according to their bulk chemistry [5, 6]. The content of metallic iron in H, L and LL groups of ordinary chondrites is 15–19 wt.%, 4–10 wt.% and 1–3 wt.%, respectively, while the content of total iron in these groups is in the ranges of $\sim$ 25–28 wt.%, $\sim$ 20–25 wt.% and $\sim$ 19–22 wt.%, respectively [7]. Ordinary chondrites formation resulted from collisions and impacts of their parent bodies in space accompanied by a variety of extreme factors like reheating, re-melting, slow cooling, etc. As the result, the features of crystal structure of various ordinary chondrites phases may reflect any differences related to the parent bodies formation as well as ordinary chondrites space history. Therefore, a comparison of structural and physical properties of iron-bearing phases in different ordinary chondrites is of interest.

In the course of Mössbauer studies of ordinary chondrites the problem of correct spectra fits arose due to the necessity to fit troilite magnetic sextet using the full static Hamiltonian (see [8–12]), otherwise a significant misfits did not allow to extract reliable parameters for the minor iron-bearing phases [13, 14]. It was shown earlier that the application of a new model of troilite component fit by simulation of the full static Hamiltonian demonstrated good results for the Mössbauer spectra of ordinary chondrites [15, 16]. Moreover, the values of Mössbauer parameters appeared to be almost the same or very close to those obtained using the full static Hamiltonian. Thus, owing to troubles with the fit of the Mössbauer spectra of ordinary chondrites with the full static Hamiltonian for troilite sextet due to a very poor convergence of procedure (we were able to fit well four spectra only [13, 14]), this new much simpler approach was used for more detailed fits of the Mössbauer spectra of fifteen fragments of ordinary chondrites from H, L and LL groups in order to reveal new minor iron-bearing phases and carry out a comparative analysis of these fragments.

## 2 Experimental

Fifteen fragments of H, L and LL ordinary chondrites such as Ochansk H4, Richardton H5, Vengerovo H5, Zvonkov H6, Saratov L4, Farmington L5, Mbale L5/6, Mount Tazerzait L5, Tsarev L5, Kunashak L6 and Chelyabinsk LL5 fragments with different lithology (No 1 and No 1a with light lithology, No 2 and No 2a with mixed light and dark lithology and No 3 with black lithology) were chosen for comparative study. These fragments were polished for the investigation using optical microscopy and scanning electron microscopy (SEM) with energy dispersion spectroscopy (EDS). Then powders from the fragments' surfaces were prepared for X-ray diffraction (XRD). After XRD analysis powdered samples were glued on Al-foil free from iron with a thickness of 6–10 mg Fe/cm$^2$ for Mössbauer measurements.

Analysis of meteorites microstructure was done using Axiovert 40 MAT optical microscope (Carl Zeiss). X-ray diffraction patterns were measured using XRD–7000 powder diffractometer (Shimadzu) operated at 40 kV and 30 mA with Ni-filtered Cu$K_\alpha$ radiation. For detailed X-ray line profile analysis, step-scan data were recorded for these samples in the $2\Theta$ range of 14–100° ($2\Theta$ steps were 0.026° or 0.030° and counting time was 25 s). SEM analysis was carried out using ΣIGMA VP electron microscope (Carl Zeiss) with an X-max

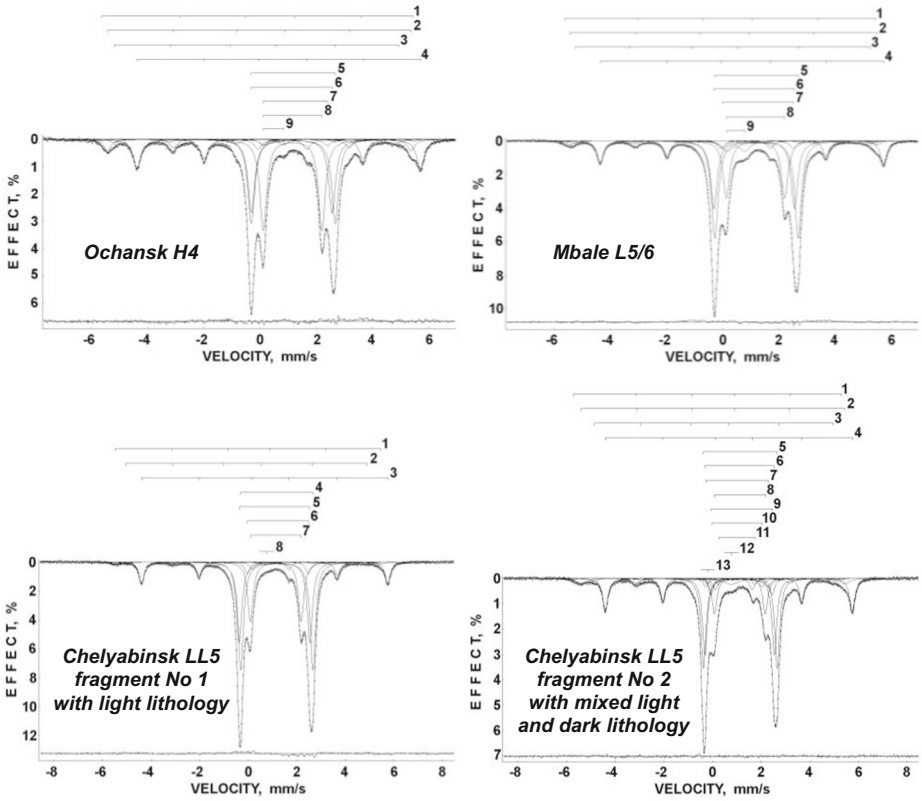


**Fig. 1** Mössbauer spectra of selected fragments of H, L and LL ordinary chondrites measured at 295 K. Indicated components are the results of the best fits with parameters listed in Table 1. Differential spectra are shown below

(Oxford Instruments) energy dispersion spectroscopy device and AMRAY 1830 scanning electron microscope equipped with EDAX PV9800 energy dispersive spectrometer.

Mössbauer spectra were measured using an automated precision Mössbauer spectrometric system built on the base of the SM-2201 spectrometer with a saw-tooth shape velocity reference signal formed by the digital-analog converter using discretization of $2^{12}$ (quantification using 4096 steps) and liquid nitrogen cryostat with moving absorber. Details and characteristics of this spectrometer and the system were given elsewhere [17–19]. The $1.8\times 10^9$ Bq$^{57}$Co(Rh) source (Ritverc GmbH, St. Petersburg) was used at room temperature. The Mössbauer spectra were measured in the cryostat with moving absorber at 295 K in transmission geometry and recorded in 4096 channels. Then all measured spectra were converted into 1024 channels by a consequent summation of four neighboring channels to increase a signal-to-noise ratio for the minor spectral components. Statistical count rates in the 1024-channel Mössbauer spectra of ordinary chondrites were in the range $3.2 \times 10^6 - 28.0 \times 10^6$ counts per channel and signal-to-noise ratio for these spectra ranged between 174 and 476.

The Mössbauer spectra of ordinary chondrites were computer fitted with the least squares procedure using UNIVEM-MS program (Institute of Physics, The Southern Federal University, Rostov-on-Don, Russian Federation) with a Lorentzian line shape. The spectral

**Table 1** Mössbauer parameters for the iron-bearing phases revealed in the Mössbauer spectra of selected ordinary chondrites shown in Fig. 1

| Sample | Γ,mm/s | δ,mm/s | $\Delta E_Q$,mm/s | $H_{eff}$,kOe | A[a],% | Component[b] |
|---|---|---|---|---|---|---|
| Ochansk H4 | 0.315±0.028 | 0.141±0.019 | −0.448±0.041 | 343.8±1.5 | 0.97 | $\alpha_2$-Fe(Ni,Co) (1) |
| | 0.315±0.028 | 0.015±0.014 | −0.070±0.014 | 334.9±0.5 | 7.09 | $\alpha$-Fe(Ni,Co) (2) |
| | 0.315±0.028 | −0.190±0.014 | 0.136± 0.020 | 313.8±0.6 | 2.14 | $\gamma$-Fe(Ni,Co) (3) |
| | 0.331±0.028 | 0.752± 0.014 | *ND*[c] | 312.6±0.5 | 18.14 | Troilite (4) |
| | 0.293±0.028 | 1.186± 0.014 | 2.985± 0.014 | – | 23.14 | Olivine M1 (5) |
| | 0.293±0.028 | 1.134± 0.014 | 2.869± 0.014 | – | 20.20 | Olivine M2 (6) |
| | 0.293±0.028 | 1.259± 0.018 | 2.293± 0.014 | – | 1.69 | Orthopyroxene M1 (7) |
| | 0.293±0.028 | 1.164± 0.014 | 2.082± 0.014 | – | 24.91 | Orthopyroxene M2 (8) |
| | 0.326[d] | 0.486± 0.022 | 0.714± 0.043 | – | 1.71 | $Fe^{3+}$ (9) |
| Mbale L5/6 | 0.290±0.028 | 0.041±0.014 | −0.279±0.025 | 343.6±0.8 | 1.16 | $\alpha_2$-Fe(Ni,Co) (1) |
| | 0.290±0.028 | 0.039±0.014 | −0.038±0.014 | 339.3±0.5 | 3.02 | $\alpha$-Fe (Ni,Co) (2) |
| | 0.290±0.028 | −0.144±0.014 | 0.288±0.014 | 325.8±0.5 | 2.20 | $\gamma$-Fe(Ni,Co) (3) |
| | 0.286±0.028 | 0.759±0.014 | *ND*[c] | 313.2±0.5 | 14.91 | Troilite (4) |
| | 0.284±0.028 | 1.199±0.014 | 2.963±0.014 | – | 31.29 | Olivine M1 (5) |
| | 0.284±0.028 | 1.119±0.014 | 2.869±0.014 | – | 21.83 | Olivine M2 (6) |
| | 0.284±0.028 | 1.257±0.014 | 2.504±0.014 | – | 2.44 | Orthopyroxene M1 (7) |
| | 0.284±0.028 | 1.166±0.014 | 2.075±0.014 | – | 18.36 | Orthopyroxene M2 (8) |
| | 0.431[d] | 0.463±0.014 | 0.643±0.014 | – | 4.80 | $Fe^{3+}$ (9) |
| Chelyabinsk | 0.341[d] | 0.005±0.017 | −0.043±0.019 – | 339.7±0.7 | 1.98 | $\alpha$-Fe(Ni,Co) (1) |
| LL5 No 1 | 0.341[d] | −0.156±0.017 | 0.158±0.032 | 308.6±0.9 | 1.50 | $\gamma$-Fe(Ni,Co) (2) |
| (Light | 0.258±0.033 | 0.747±0.017 | *ND*[c] | 314.9±0.5 | 13.25 | Troilite (3) |
| lithology) | 0.264±0.033 | 1.180±0.017 | 2.969±0.017 | – | 34.29 | Olivine M1 (4) |
| | 0.264±0.033 | 1.083±0.017 | 2.913±0.017 | – | 25.68 | Olivine M2 (5) |
| | 0.264±0.033 | 1.219±0.017 | 2.523±0.017 | – | 3.66 | Orthopyroxene M1 (6) |
| | 0.264±0.033 | 1.132±0.017 | 2.091±0.017 | – | 18.82 | Orthopyroxene M2 (7) |
| | 0.640±0.081 | 0.756[d] | – | – | 0.83 | Chromite (8) |
| Chelyabinsk | 0.240±0.087 | −0.096±0.025 | −0.220±0.050 | 341.2±1.3 | 0.85 | $\alpha_2$-Fe(Ni,Co) (1) |
| LL5 No 2 | 0.467±0.033 | 0.024±0.017 | −0.003±0.021 | 336.5±0.5 | 6.41 | $\alpha$-Fe(Ni,Co) (2) |
| (mixed light | 0.372±0.033 | −0.029±0.017 | 0.155±0.029 | 304.6±1.0 | 2.30 | $\gamma$-Fe(Ni,Co) (3) |
| and dark | 0.262±0.033 | 0.756±0.017 | *ND*[c] | 315.1±0.5 | 19.77 | Troilite (4) |
| lithology) | 0.238±0.033 | 1.147±0.017 | 3.032±0.017 | – | 25.04 | Olivine M1 (5) |
| | 0.238±0.033 | 1.119±0.017 | 2.856±0.017 | – | 21.28 | Olivine M2 (6) |
| | 0.238±0.033 | 1.003±0.017 | 2.563±0.030 | – | 2.45 | Orthopyroxene M1 (7) |
| | 0.238±0.033 | 1.125±0.017 | 2.089±0.017 | – | 9.89 | Orthopyroxene M2 (8) |
| | 0.238±0.033 | 1.199±0.017 | 2.516±0.017 | – | 4.57 | Clinopyroxene M1 (9) |
| | 0.238±0.033 | 1.011±0.017 | 2.049±0.017 | – | 2.41 | Clinopyroxene M2 (10) |
| | 0.238±0.033 | 0.997±0.017 | 1.480±0.017 | – | 1.73 | Hercynite (11) |
| | 0.776±0.034 | 0.777±0.017 | – | – | 2.69 | Chromite (12) |
| | 0.233±0.034 | −0.191±0.043 | – | – | 0.60 | $\gamma$-Fe(Ni, Co) par. (13) |

[a]Relative areas are given with two decimal digits as calculated to keep 100 % of total area.

[b]Numbers in parenthesis correspond to the spectral components in Fig. 1. [c]Not determined. [d]Fixed parameter.

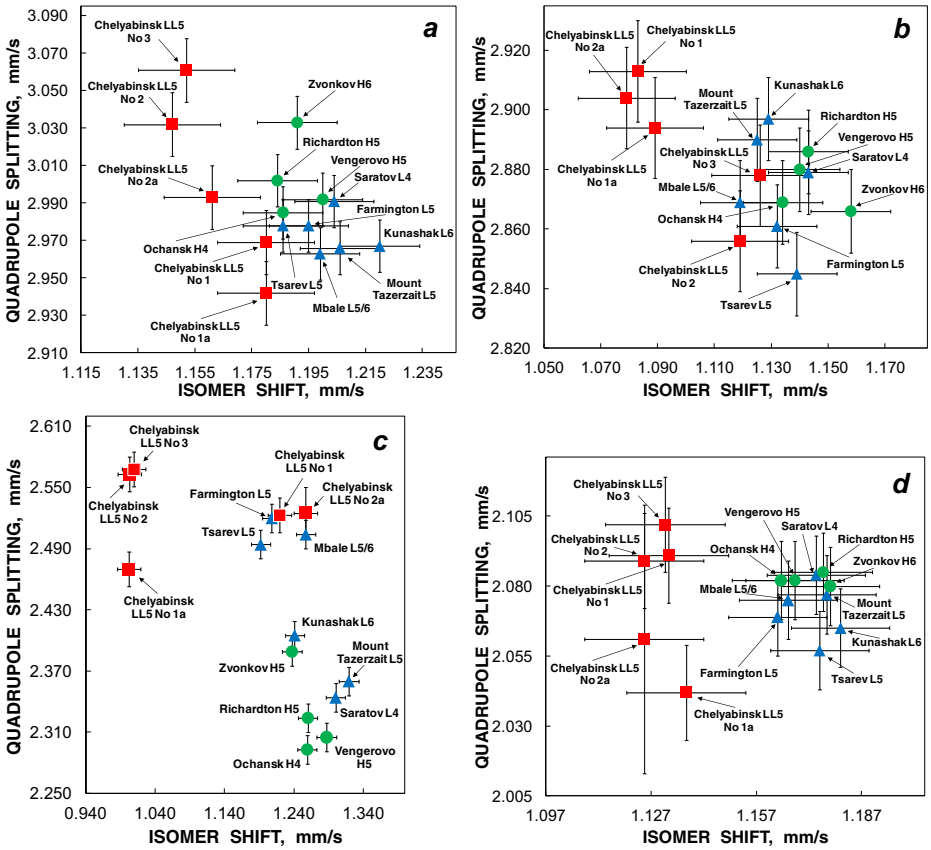


**Fig. 2** The plots of the $^{57}$Fe hyperfine parameters for the M1 (**a**) and M2 (**b**) sites in olivine and the M1 (**c**) and M2 (**d**) sites in orthopyroxene for ordinary chondrites from H ●, L ▲ and LL ■ groups

parameters such as: isomer shift, $\delta$, quadrupole splitting (quadrupole shift for magnetically split components), $\Delta E_Q$, magnetic hyperfine field, $H_{eff}$, line width, $\Gamma$, relative area of spectral components, A, and statistical criterion, $\chi^2$, were determined. The Mössbauer spectrum of standard absorber of $\alpha$-Fe foil (7 $\mu$m) demonstrated Lorentzian line shape with the values of $\Gamma_{1-6} = 0.238 \pm 0.031$ mm/s, $\Gamma_{2-5} = 0.232 \pm 0.031$ mm/s and $\Gamma_{3-4} = 0.224 \pm 0.031$ mm/s. An instrumental (systematic) error for each spectrum point was $\pm$ 0.5 channel (in mm/s), the instrumental (systematic) error for the hyperfine parameters was $\pm$ 1 channel (in mm/s or kOe). If statistical error calculated with the fitting procedure (fitting error) for these parameters exceeded the instrumental (systematic) error we used the larger error instead. Criteria for the best fits were differential spectrum, $\chi^2$ and a physical meaning of the spectral parameters. Values of $\delta$ are given relative to $\alpha$-Fe at 295 K.

## 3 Results and discussion

Microstructure analysis of all studied fragments using optical microscopy showed that metallic grains and troilite inclusions are located in silicate matrix. Some few grains of

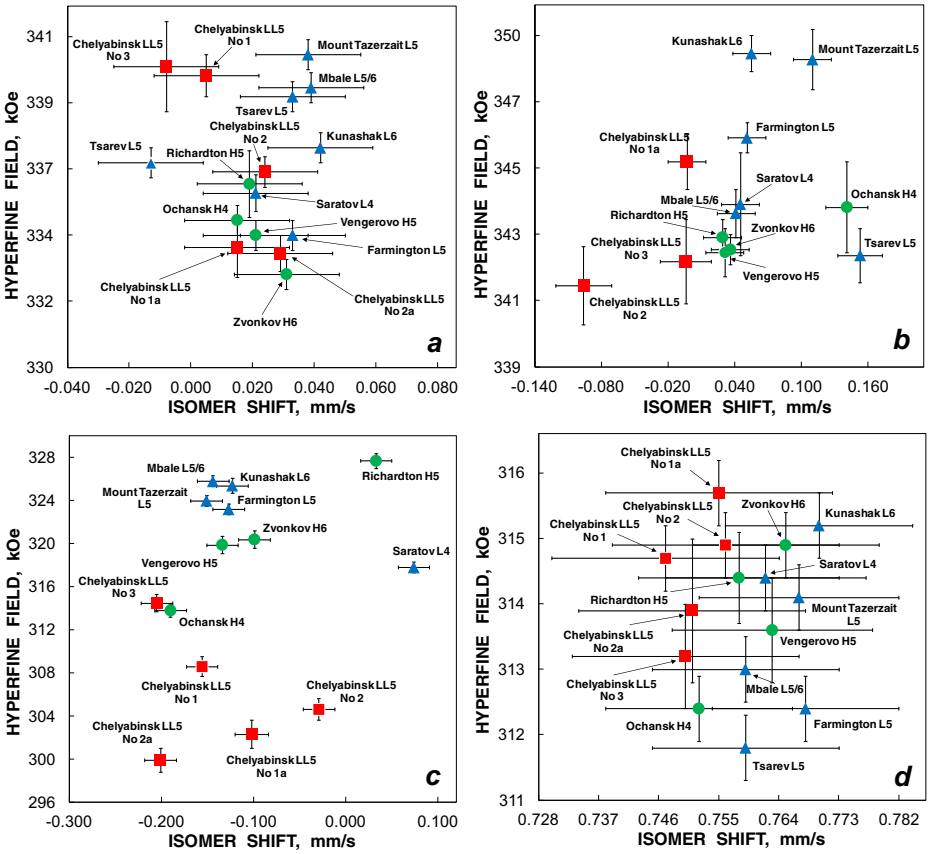


**Fig. 3** The plots of the $^{57}$Fe hyperfine parameters for $\alpha$-Fe(Ni, Co) (**a**), $\alpha_2$-Fe(Ni, Co) (**b**) and $\gamma$-Fe(Ni, Co) (**c**) phases and troilite (***d***) in ordinary chondrites from H ●, L ▲ and LL ■ groups

chromite were observed in all Chelyabinsk LL5 fragments and some other ordinary chondrites from H and L groups. XRD data were reconsidered taken into account well-known data about ordinary chondrites. The content of iron-bearing phases appeared to be different in different ordinary chondrites fragments. The minor iron-bearing phases such as clinopyroxene, chromite, hercynite $FeAl_2O_4$ were revealed from the XRD data in Chelyabinsk LL5 fragments No 1a, 2, 2a and 3 only. Ilmenite $FeTiO_3$ was revealed from the XRD data for Chelyabinsk LL5 fragment No 2a only while chromite only was found in the XRD data for Chelyabinsk LL5 fragment No 1. These results were confirmed by SEM with EDS analysis detected mentioned minor iron-bearing phases in studied ordinary chondrites also.

Mössbauer spectra of ordinary chondrites from H, L and LL groups measured at room temperature were fitted well using new model with the full Hamiltonian simulation for troilite magnetic sextet using three doublets (details can be found elsewhere [15, 16]). The results of the best fits of the selected Mössbauer spectra of Ochansk H4, Mbale L5/6 and Chelyabinsk LL5 (fragments No 1 with light lithology and No 2 with mixed light and dark lithology) are shown in Fig. 1. Mössbauer parameters of spectral components revealed in these Mössbauer spectra fits and related to corresponding iron-bearing phases are given in Table 1. Number of spectral components revealed in different Mössbauer spectra of

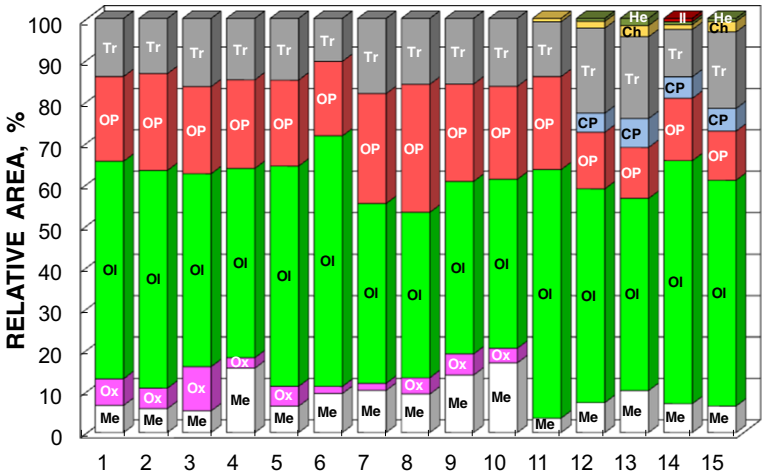


**Fig. 4** Comparison of the relative areas of components revealed in the Mössbauer spectra of ordinary chondrites from H, L and LL groups: 1 – Saratov L4, 2 – Mount Tazerzait L5, 3 – Tsarev L5, 4 – Farmington L5, 5 – Mbale L5/6, 6 – Kunashak L6, 7 – Ochansk H4, 8 – Richardton H5, 9 – Vengerovo H5, 10 – Zvonkov H6, 11 – Chelyabinsk LL5 No 1, 12 – Chelyabinsk LL5 No 1a, 13 – Chelyabinsk LL5 No 2, 14 – Chelyabinsk LL5 No 2a, 15 – Chelyabinsk LL5 No 3; Me – metallic iron, Ox – ferric compound (weathering product), Ol – olivine, OP – orthopyroxene, CP – clinopyroxene, Tr – troilite, Ch – chromite, He – hercynite, Il – ilmenite

studied fragments was different. It should be noted that the spectral components corresponding to the M1 and M2 sites in clinopyroxene, chromite, hercynite, ilmenite and paramagnetic $\gamma$-Fe(Ni, Co) phase were revealed in Mössbauer spectra of Chelyabinsk LL5 meteorite fragments only. This was a result of the weathering of H and L ordinary chondrites in contrast to fresh Chelyabinsk LL5 fragments. Therefore, a larger contribution of paramagnetic $Fe^{3+}$ component in the spectra of the former meteorites (component 9 in Fig. 1a, b) hid the minor paramagnetic components related to chromite, hercynite and paramagnetic $\gamma$-Fe(Ni, Co) phase that is why these components were not revealed during the fits.

Using the $^{57}$Fe hyperfine parameters for the M1 and M2 sites in olivine and orthopyroxene it is possible to compare these silicates in studied fragments (Fig. 2). Small differences in the $^{57}$Fe hyperfine parameters for different ordinary chondrites as well as for different fragments of Chelyabinsk LL5 meteorite could be related to small variations in the $^{57}$Fe local microenvironment in these silicate crystals. A comparison of the $^{57}$Fe hyperfine parameters for $\alpha$-Fe(Ni, Co), $\alpha_2$-Fe(Ni, Co) and $\gamma$-Fe(Ni, Co) phases and troilite in the studied meteorites are shown in Fig. 3. The differences in the hyperfine field values and isomer shift for each $\alpha$-Fe(Ni, Co), $\alpha_2$-Fe(Ni, Co) and $\gamma$-Fe(Ni, Co) phase in different ordinary chondrites may be related to small variations in Ni and Co concentrations in the metallic grains. Values of $H_{eff}$ for troilite component obtained using the simulation of full static Hamiltonian appeared to be also slightly different for some meteorites. The distinctions in hyperfine field values may indicate the deviation from stoichiometry of troilite in the studied fragments as a possible result of reheating and/or re-melting.

The relative areas of spectral components permitted us to evaluate roughly the content of various iron-bearing minerals in different ordinary chondrites. The comparison of different iron-bearing phases is shown in Fig. 4. The content of the relative part of iron in the same phases of ordinary chondrites appeared to be different in various fragments that may reflect different phase composition in the parent bodies. For instance, olivine content in H ordinary

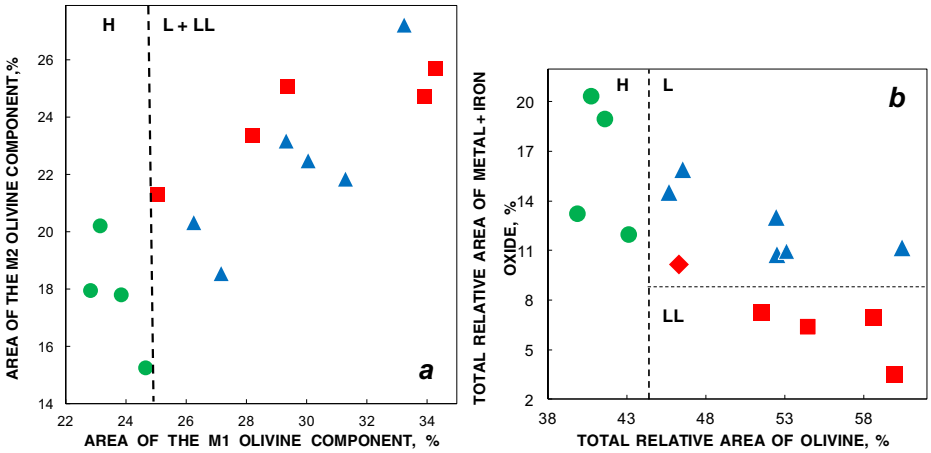


**Fig. 5** The possibilities of ordinary chondrites classification using the total relative areas for the M1 and M2 olivine spectral components (**a**) and for metallic + oxidized iron and olivine spectral components (**b**): H ●, L ▲ and LL ■ groups, ◆ is Chelyabinsk LL5 fragment No 2

chondrites is smaller than that in L and LL chondrites that corresponds to the well-known data for content of the iron-rich end-member of the olivine solid-solution: 16–20 mol.%, 22–26 mol.% and 27–31 mol.% for H, L and LL groups, respectively [7]. Therefore, there were attempts to use Mössbauer parameters for distinguishing ordinary chondrites from different groups for their classification [20–22].

Examples of evaluation of ordinary chondrites classification using Mössbauer parameters are shown in Fig. 5. The plot of the relative areas of spectral components related to the M1 and M2 sites in olivine showed the possibility to distinguish all studied fragments into two groups H and L+LL (Fig. 5a). A conventional border between these two groups can be considered at the relative area of component related to the M1 sites in olivine equal to $\sim 25$ %. Further comparison of the relative areas of components related to metallic iron and olivine is more interesting. However, in this case the total relative areas of the Mössbauer spectral components related to metallic iron could be considered roughly as a sum of the areas of metallic iron components and oxidized iron component for weathered chondrites with a low weathering grade. The plot of the total relative areas for metallic iron + oxidized iron components and for olivine M1 and M2 components is shown in Fig. 5b. This plot allows distinguishing different H, L and LL ordinary chondrites. It was interesting to find Chelyabinsk LL5 fragment No 2 in the region corresponding to L chondrites due to much higher content of metallic iron than that in other fragments of Chelyabinsk LL5 meteorite. This fact may be a result of breccia structure of Chelyabinsk LL5 meteorite formed by collisions of different parent bodies in space.

## 4 Conclusion

Mössbauer spectra of ordinary chondrites from H, L and LL groups measured with a high velocity resolution at 295 K were much better fitted using simulation of the full static Hamiltonian for troilite magnetic sextet fit that decreased spectra misfits and permitted revealing the minor iron-bearing phases in fresh Chelyabinsk LL5 meteorite fragments. In

the Mössbauer spectra of weathered H and L ordinary chondrites it was impossible due to overlapping of ferric component and components which can be related to chromite, hercynite, ilmenite and paramagnetic $\gamma$-Fe(Ni, Co) phase. Small variations of the hyperfine parameters were observed for the same iron-bearing phases in both different ordinary chondrites and different fragments of Chelyabinsk LL5 meteorite. This may indicate the small variations in the $^{57}$Fe local microenvironments for some iron-bearing minerals due to different thermal and impact history of these meteorites. Relative areas of the Mössbauer spectral components related to metallic iron (and ferric compound in weathered meteorites) and to the M1 and M2 sites in olivine can be used for ordinary chondrites classification.

**Acknowledgments** The authors thank Dr. A.V. Chukin (Institute of Physics and Technology, Ural Federal University, Ekaterinburg) for XRD measurements, G.A. Yakovlev (Institute of Physics and Technology, Ural Federal University, Ekaterinburg) and Z. Bendő (Department of Petrology and Geochemistry, Institute of Geography and Earth Sciences, Eötvös Loránd University, Budapest) for SEM with EDS measurements. This work was supported in part by the Ministry of Education and Science of Russian Federation (basic financing for the Project # 2085), by Act 211 Government of the Russian Federation, contract № 02.A03.21.0006 and the RFBR project No 15-35-21164 mol_a_ved. Contribution to the study from A.A.M. was funded by the RFBR according to the research project No 16-32-00151 mol_a.

## References

1. Verma, H.C., Rawat, A., Paliwal, B.S., Tripathi, R.P.: Hyperfine Interact. **142**, 643–652 (2002)
2. Al-Rawas, A.D., Gismelseed, A.M., Yousif, A.A., Elzain, M.E., Worthing, M.A., Al-Kathiri, A., Gnos, E., Hofmann, B.A., Steele, D.A.: Planet. Space Sci. **55**, 859–863 (2007)
3. Cadogan, J.M., Rebbouh, L., Mills, J.V.J., Bland, P.A.: Hyperfine Interact. **222**(2), S91—S98 (2013)
4. Gałłazka-Friedman, J., Szlachta, K., Karwowski, Ł., Woźniak, M.: Hyperfine Interact. **226**, 593–600 (2014)
5. Dodd Jr., R.T., Van Schmus, W.R.: J. Geophys. Res. **70**, 3801–3811 (1965)
6. Van Schmus, W.R., Wood, J.A.: Geochim. Cosmochim. Acta. **31**, 747–765 (1967)
7. Dodd, R.T.: Meteorites: A Petrological-Chemical Synthesis, p. 368. Cambridge University Press, Cambridge (1981)
8. Kruse, O., Ericsson, T.: Phys. Chem. Minerals **15**, 509–513 (1988)
9. Kruse, O.: Am. Mineral. **75**, 755–763 (1990)
10. Grandjean, F., Long, G.J., Hautot, D., Whitney, D.L.: Hyperfine Interact. **116**, 105–115 (1998)
11. Forder, S.D., Bland, P.A., Galazka–Friedman, J., Urbanski, M., Gontarz, Z., Milczarek, M., Bakun–Czubarow, N.: Hyperfine Interact. C **5**, 405–408 (2001)
12. Oshtrakh, M.I., Klencsár, Z., Petrova, E.V., Grokhovsky, V.I., Chukin, A.V., Shtoltz, A.K., Maksimova, A.A., Felner, I., Kuzmann, E., Homonnay, Z., Semionkin, V.A.: Mat. Chem. Phys. **174**, 100–111 (2016)
13. Maksimova, A.A., Oshtrakh, M.I., Klencsár, Z., Petrova, E.V., Grokhovsky, V.I., Kuzmann, E., Homonnay, Z., Semionkin, V.A.: J. Mol. Struct. **1073**, 196–201 (2014)
14. Oshtrakh, M.I., Maksimova, A.A., Klencsár, Z., Petrova, E.V., Grokhovsky, V.I., Kuzmann, E., Homonnay, Z., Semionkin, V.A.: J. Radioanal. Nucl. Chem. **308**, 1103–1111 (2016)
15. Maksimova, A.A., Klencsár, Z., Oshtrakh, M.I., Petrova, E.V., Grokhovsky, V.I., Kuzmann, E., Homonnay, Z., Semionkin, V.A.: Hyperfine Interact. **237**, 33 (2016)
16. Maksimova, A.A., Oshtrakh, M.I., Petrova, E.V., Grokhovsky, V.I., Semionkin, V.A.: Spectrochim. Acta A Mol. Biomol. Spectrosc. (2016). doi:10.1016/j.saa.2016.04.032
17. Oshtrakh, M.I., Semionkin, V.A., Milder, O.B., Novikov, E.G.: J. Radioanal. Nucl. Chem. **281**, 63–67 (2009)
18. Semionkin, V.A., Oshtrakh, M.I., Milder, O.B., Novikov, E.G.: Bull. Rus. Acad. Sci. Phys. **74**, 416–420 (2010)
19. Oshtrakh, M.I., Semionkin, V.A.: Spectrochim. Acta A Mol. Biomol. Spectrosc. **100**, 78–87 (2013)
20. Paliwal, B.S., Tripathi, R.P., Verma, H.C., Sharma, S.K.: Meteorit. Planet. Sci. **35**, 639–642 (2000)
21. Verma, H.C., Jee, K., Tripathi, R.P.: Meteorit Planet. Sci. **38**, 963–967 (2003)
22. Oshtrakh, M.I., Petrova, E.V., Grokhovsky, V.I., Semionkin, V.A.: Meteorit. Planet. Sci. **43**, 941–958 (2008)